

Ellipsometry and structure studies of chromium, molybdenum, and platinum silicides

Juh-Tzeng Lue and Shean-Jyeh Mu

Department of Physics, National Tsing Hua University, Hsinchu, Taiwan, Republic of China

In-Chin Wu

Materials Science Center, National Tsing Hua University, Hsinchu, Taiwan, Republic of China

(Received 8 January 1987; revised manuscript received 30 March 1987)

The surface morphologies and structural phases of CrSi₂, MoSi₂, and PtSi are investigated using a transmission electron microscope. Epitaxial PtSi and polycrystalline CrSi₂ and MoSi₂ are formed by rapid thermal annealing and conventional thermal annealing, respectively. The complex refractive indices are determined using a polychromatic ellipsometer at wavelengths of 400 to 700 nm.

I. INTRODUCTION

Despite the technical importance of transition-metal silicides in very-large-scale integration (VLSI) electronics, little is known about the optical constants $N = n - ik$ of these materials. However, due to their high potential for application in optoelectronic devices,¹ a better understanding of their properties would be highly desirable.

In previous papers^{2,3} we have successfully determined the optical constants of thin films of Ni/Si and Pd/Si systems using a polychromatic ellipsometer. In the present work we report the values of n and k for three silicide systems (CrSi₂, MoSi₂ and PtSi) using the same method. Both the morphology and the phase identification of these silicides were investigated by use of a transmission electron microscope (TEM). A modified Drude model is used to explain the experimental data. For the Pt/Si system, the rapid thermal annealing (RTA) method is applied to attain a stable PtSi which can be epitaxially grown on the silicon substrates in forms of Pt(010)//Si(111) and PtSi[001]//Si⟨110⟩ (where // represents an orientation relationship between epilayer and substrate). For the Cr/Si and Mo/Si systems, the annealing was done isothermally at 900°C for 1 h in an oil-free high-vacuum chamber. The final stable phases are polycrystalline C40 CrSi₂ and hexagonal C40 and tetragonal C11b MoSi₂, respectively. All of the refractive indices are rather flat within the visible range and the values of n and k have a tendency to approach each other for the Pt and Cr silicides after annealing, whereas for MoSi₂ n and k separate further as compared with their virgin-film values.

II. EXPERIMENTAL PROCEDURES

Silicon wafers of 3–10 Ω cm with ⟨111⟩ and ⟨001⟩ orientations were first cleaned chemically by the usual procedures.⁴ The samples were etched in a buffered HF solution (HF:H₂O=1:50) for 2 min and then dried with a pressurized nitrogen gun immediately before being loaded into the electron-gun-deposition system.

Metal thin films of 300–400 Å in thickness were electron gun deposited onto silicon substrates at room tem-

perature. The deposition rate was about 2 Å/s under a pressure of 2×10^{-6} Torr. For the Pt/Si system, the deposited samples were annealed in a Perkin-Elmer HGA-300 graphite furnace at 900°C for 100 s (Ref. 5) in an ambience of high-purity Ar gas. For the Cr/Si and Mo/Si systems, all the deposited samples were annealed at 900°C for 1 h in an oil-free vacuum furnace under a pressure below 1×10^{-6} Torr.

In order to prevent the deposited film from oxidation and/or contamination during heat treatment, all samples were stacked with metal films facing each other.^{6,7} Such a configuration is referred to as a “face-to-face” arrangement. For samples annealed with this arrangement, their surfaces have a uniform, shiny optical appearance.

Before taking ellipsometry measurement, all annealed samples were stored in a vacuum chamber to prevent contamination. The morphologies and phases of silicide films were characterized by use of a transmission electron microscope (TEM). Randomly oriented particles will give diffraction rings lying in a cone with apex angle $4\theta_{hkl}$ centered on the incident beam direction, satisfying the Bragg law⁸

$$n\lambda = 2d_{hkl}\sin\theta_{hkl}, \quad (1)$$

where $n\lambda$ is an integral number of electron-beam wavelengths, and d_{hkl} is the interplanar spacing for the $\{hkl\}$ planes. An epitaxial layer or highly oriented polycrystalline particles will give spot patterns corresponding to magnified images of planar sections through the reciprocal lattice. For the silicide compounds, phase identification was done by indexing the selected-area diffraction (SAD) patterns using internal (Si: d_{220}) calibration data for obtaining the camera length. The errors in these experimental d spacings are within 3% as compared with the American Society for Testing and Materials (ASTM) x-ray diffraction cards. Analysis of the direct images and diffraction patterns revealed unambiguously the presence of single-phase epitaxial PtSi and polycrystalline CrSi₂ and MoSi₂ which uniformly cover the surface of the silicon substrates without evidence of island formation.

The refractive indices of PtSi, CrSi₂, and MoSi₂ are measured by a polychromatic ellipsometer as described in

previous work.³ Samples annealed by this face-to-face arrangement are free from oxidation as examined by the Auger spectrum and showing a smooth mirror reflection. Therefore a single air-material model can be used to solve the data from the ellipsometry extinction parameters.

III. EXPERIMENTAL RESULTS

A. Pt/Si system

The as-deposited Pt film on the Si(111) substrate with a thickness of 300 Å shows a fine crystalline structure with grain sizes of about 200 Å. The values of n and k measured by the ellipsometer as shown in Fig. 1, indicate a tendency of $k \gg n$. The discrepancy between this work and others⁹ is about 10% as can be seen on the same chart. This can be expected since different deposition methods and different substrates can introduce unlike surface morphologies and optical reflectivities. The reflectivity inserts in the same figure indicating a value lying between 60% and 70% over the visible range.

The as-deposited Pt film on the silicon substrate can be completely transformed into PtSi (orthorhombic MnP type) after 900°C for 100-s rapid thermal annealing. Epitaxial growth of the PtSi silicide overlayer is found on the Si(111) substrate which can be checked by the appearance of a pseudohexagonal spot pattern as shown in the inset of Fig. 2. The epitaxial relationships were determined to be PtSi(010)//Si(111), and PtSi[001]//Si[220].¹⁰ There are three variants of PtSi grains in the silicide layer. Every variant with 0.15 μm in average size is preferably oriented with the same epitaxial symmetry resulting in a spot TEM diffraction pattern.

The optical constants as shown in Fig. 3 reveal lower values of n and higher values of k for Pt silicide than those of the as-deposited Pt film. In the same chart, we find that the reflectivities for PtSi and Pt film are 0.40 and 0.50, respectively.

B. Cr/Si system

Metal Cr of 400 Å in thickness was deposited on a *p*-type Si(001) substrate. Randomly oriented Cr grains of 200 Å in grain size were observed in this sample. Optical

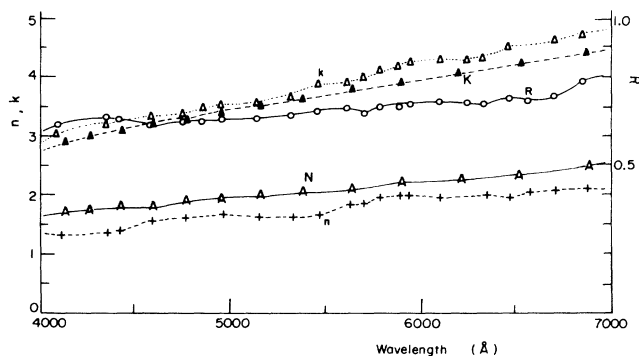


FIG. 1. Values of n and k for as-deposited Pt/Si of 300 Å, the data from Ref. 9 are denoted by N and K . The reflectivity R is also plotted on the same chart.

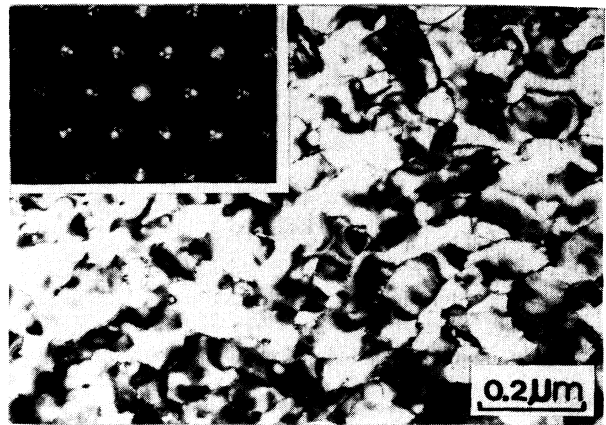


FIG. 2. Bright-field (BF) micrograph of PtSi on Si(111) for 900°C, 100 s annealed; inset is the diffraction pattern (DP). The grain size is about 0.15 μm.

constants as shown in Fig. 4 also have the tendency of $k \gg n$. The Cr thin film appears silvery shining. The normal-incident reflectivity is flat over the visible region as shown in the same figure. Its values are as high as Pt thin film in a range from 60% to 70%.

Polycrystalline CrSi₂ grains¹¹ of 1000 Å in average grain size are found in the samples annealed at 900°C for 1 h. Dark-field (DF) image and phase identification of CrSi₂ are shown in Figs. 5 and 6, respectively. Optical constants depicted in Fig. 7 indicate lower values of k and higher values of n than those of the as-deposited Cr film. This figure clearly shows that the values of n drastically increase at wavelengths longer than 6500 Å.

The CrSi₂ film has a silvery shining appearance, too. Its reflectivity is flat over the visible region and has values within 40% to 50% which is lower than that of the original Cr film.

C. Mo/Si system

The grain size of the as-deposited 400-Å Mo film is measured to be about 100 Å. A comparison between the measured optical constants (n and k) in a thin-film speci-

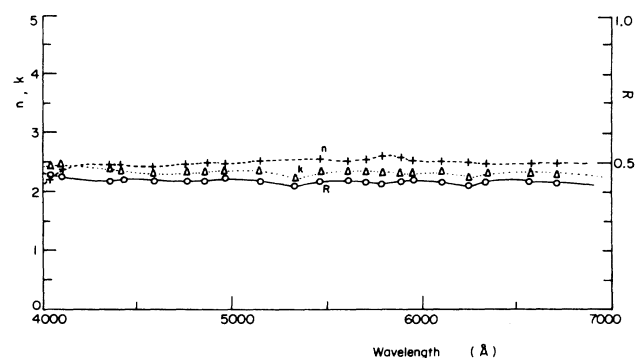


FIG. 3. Values of n , k , and R for PtSi.

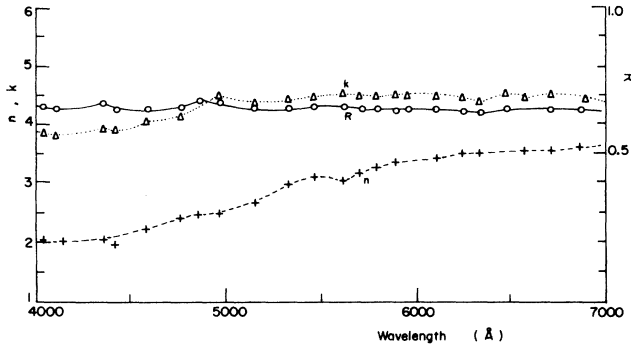


FIG. 4. Value of n , k , and R for as-deposited Cr/Si of 400 Å.

men and the published data¹² is plotted in Fig. 8. The considerable discrepancy between these values may arise from different sample preparations, in which the electron relaxation time depends on the impurity contents and grain size which inevitably will affect the optical conductivity. The reflectivity remains at about 50% in the visible region as shown in Fig. 8.

Both hexagonal $C40$ and tetragonal $C11b$ MoSi_2 (h - MoSi_2 and i - MoSi_2) were formed after 900 °C, 1 h vacuum annealing.¹³ The grains were measured to be about 1000 Å in size as shown in Fig. 9. The optical constants n and k are shown in Fig. 10. Their values are nearly flat and only slightly vary over the visible region. The values of n are greater, while the values of k are less than those of the as-deposited metallic thin film. The reflectivities appear to be no different with the as-deposited Mo films and have values about 0.50.

IV. DISCUSSIONS

The optical constants of metals can be derived from the static Hartree dielectric function by¹⁴

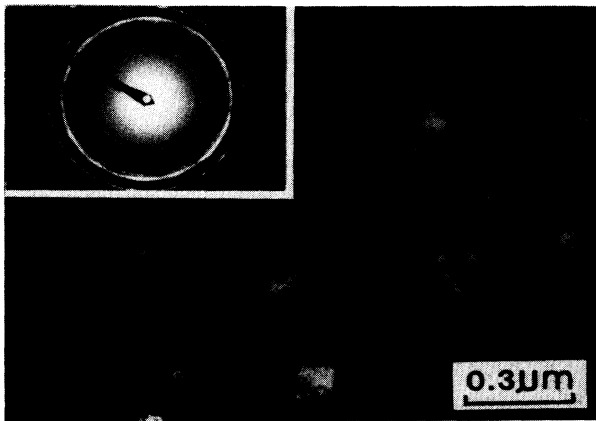


FIG. 5. Dark-field (DF) micrography of CrSi_2 on Si(001) with grain size of 0.1 μm ; inset is the DP.

$$n - ik = \sqrt{\epsilon(q, \omega)} = \left[1 - \frac{4\pi e^2}{q^2} \chi(q, \omega) \right]^{1/2} = \left[1 - \frac{4\pi e^2}{q^2} \frac{n_s}{V_t} \right]^{1/2}, \quad (2)$$

where $n_s = dn/d\xi$ is the density of states per unit energy at the Fermi energy ξ , V_t is the total applied potential, q is the photon wave number, and ω is the incident frequency. At long-wavelength limit ($q=0$), if we retain the electron relaxation and the finite incident frequency, then Eq. (1) is reduced to Drude formula as given by

$$\epsilon(q, \omega) \rightarrow 1 + \frac{4\pi i N_e e^2 \tau}{m\omega(1 - i\omega\tau)}, \quad (3)$$

where τ is the electron relaxation time and N_e is the conduction electron density. For intermetallic silicides, the conduction electrons come mostly from the metals while the silicon atoms contribute a small amount by charge transfer through p - d or p - f hybridization. This can be inspected by noting that the optical constants of silicides are modified from their original metals. Clarification of the band structures of silicides having not yet been attempted, the absorption peaks can possibly be attributed to the d -band and conduction-band transitions as given by¹⁴

$$n(q) = \sum_q \left[\frac{2 \langle -k + q | \Delta | d \rangle \langle d | \Delta | k \rangle}{(E_d - E_k)(E_k - E_{k+q})} - \frac{\langle k | \Delta | d \rangle \langle d | \Delta | k \rangle}{(E_d - E_k)^2} \right], \quad (4)$$

where Δ is the variation of pseudopotential due to electron change of valence states and d states. The above equation together with the Boltzman transport equation also gives the frequency dependence of the optical constants.

Within the visible light, we have $1/\tau \ll \omega \ll \omega_p$ for metals, where τ is the electronic relaxation time and $\omega_p = (4\pi N_e e^2/m)^{1/2}$ is the plasma frequency. The Drude model implies

$$n^2 - k^2 \approx 1 - \omega_p^2/\omega^2 \text{ and } 2nk \approx \omega_p^2\tau/\omega. \quad (5)$$

Since $\omega_p^2/\omega^2 > 1$, $n^2 - k^2$ is negative and we have $k > n$. This occurs in most noble metals. If the number of conduction electrons increases during silicide formation, then ω_p becomes larger and the discrepancy between k and n increases. On the other hand, with the loss of electrons during silicide formation, k is likely to approach n and even reverse the relative values as occurs in the semiconductors.

Charge transfer can also occur between metal and silicon during silicide formation. The total electronic charge in the i th cell atom of the α atomic orbital can be numerically calculated by the extended Huckel theory^{15,16} which specifies

$$q_{i,\alpha} = 2 \sum_k \sum_n \int_{-\infty}^{E_f} dE \delta(E - E_{nk}) B_n(k)^{-1} \times S_{ai,ai}(k) |C_{ai}(kn)|^2, \quad (6)$$

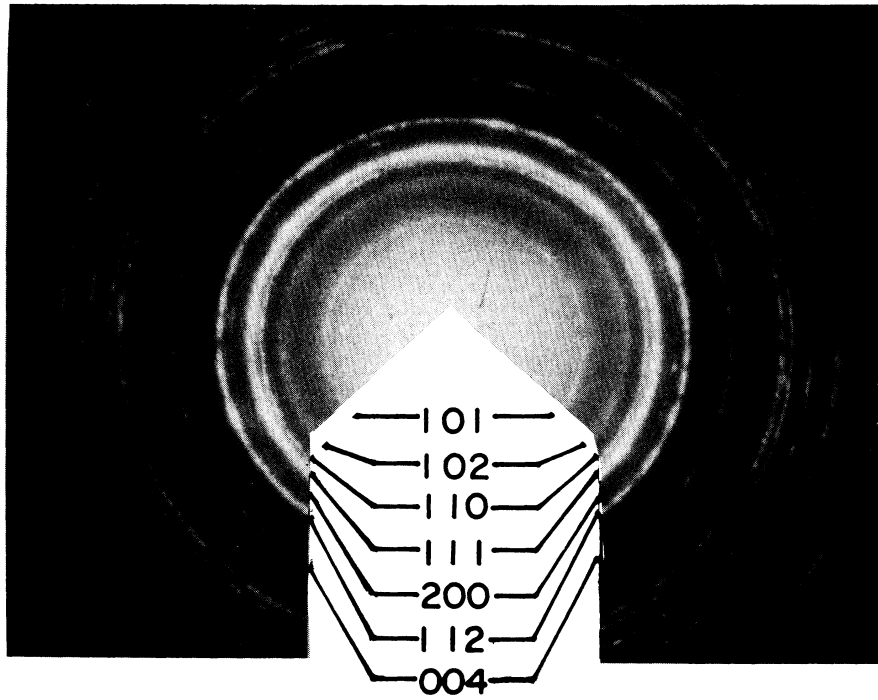


FIG. 6. A typical SAD ring pattern of CrSi₂ (1200 Å)/Si(001) implying an evidence of single phase.

where $B_n(k)$ is a normalization factor of the Slater wave function, $S_{\alpha_i, \beta_j}(k)$ is the matrix element of the overlap integrals of two Bloch wave functions $\phi_{\alpha_i}(k)$ and $\phi_{\beta_j}(k)$, and $C_{\alpha_i}(kn)$ is the proper expansion coefficient of the α th orbital to the n band. With the values of ϕ_{α_i} , B_n , and S_{α_i, β_j} one can evaluate the charge transfer. To form silicides, the $3s$ and $3p$ single δ Slater orbitals for silicon and both single and double δ orbitals for s , p and d states of metallic atoms are hybridized. The calculation implies that every Si atom loses 0.044 electrons to PtSi (Ref. 16) while Pt gains almost the same number of electrons from PtSi. If the value of total conduction electron density is the dominant effect that controls the dielectric constant,

then the reverse of the relative values of n and k of PtSi with respect to its original films will not be so prominent.

Although Pd and Pt belong to the same group of noble metals and have almost the same resistivity ($28 \mu\Omega \text{ cm}$ for PtSi and $35 \mu\Omega \text{ cm}$ for PdSi), the k of PtSi is much larger than that of PdSi (Ref. 3) implying that PtSi behaves much more like a metal. The large increase of n for MoSi₂ indicates a great reduction of conduction electrons during silicide formation which can be confirmed by the sharp increase of resistivities from Mo ($\sim 5.78 \mu\Omega \text{ cm}$) to MoSi₂ ($100 \mu\Omega \text{ cm}$). MoSi₂ has the same character of resonance transitions as occurs in NiSi₂.² The constancy of optical constants of the Cr/Si system implies that the con-

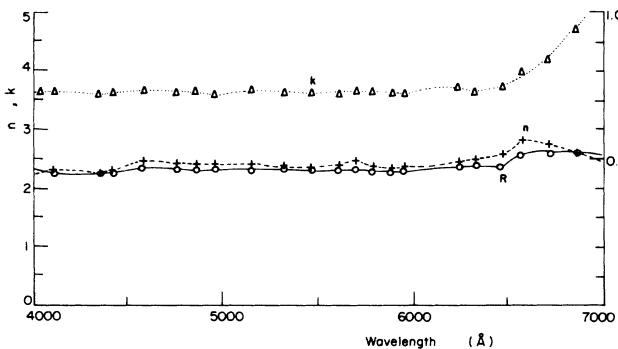


FIG. 7. Values of n , k , and R of CrSi₂.

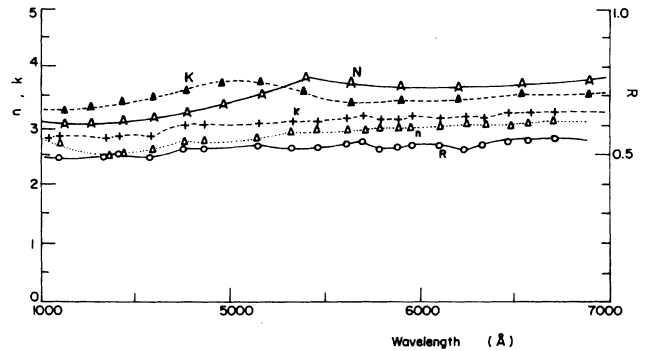


FIG. 8. Values of n , k , and R of as-deposited Mo/Si of 400 Å in thickness and 100 Å in grain size.

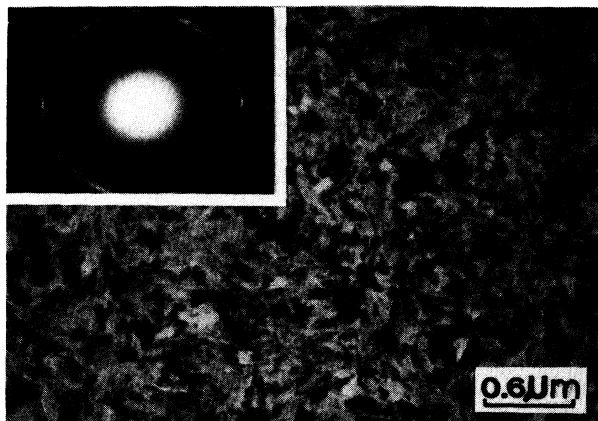


FIG. 9. BF of MoSi_2 on Si(111) with grain size of 1000 \AA ; the inset is the DP.

duction electron density is only slightly changed. Stoichiometric CrSi_2 is a p -type degenerate semiconductor with band gap of 0.3 eV (Ref. 17) and has a high resistivity of $600 \mu\Omega \text{ cm}$.

In conclusion, we have reported the optical constants of PtSi, CrSi_2 , and MoSi_2 . Their phases are carefully

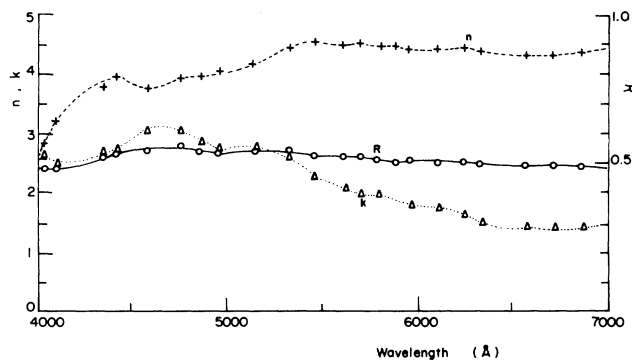


FIG. 10. Values of n , k , and R of MoSi_2 .

checked by the diffraction patterns of a transmission electron microscope. The complex refractive indices qualitatively agree with the Drude model.

ACKNOWLEDGMENT

This work was supported by the National Science Council of the Republic of China.

- ¹S. P. Murarka, *Silicides for VLSI Application* (Academic, Orlando, 1983), p. 176.
- ²H. W. Chen, and J. T. Lue, *J. Appl. Phys.* **59**, 2165 (1986).
- ³J. T. Lue, H. W. Chen, and S. I. Lew, *Phys. Rev. B* **34**, 5438 (1986).
- ⁴R. M. Burger and R. P. Donovan, *Fundamentals of Silicon Integrated Device Technology* (Research Triangle Institute, North Carolina, 1967), Vol. 1, p. 328.
- ⁵I. C. Wu, J. J. Chu, and L. J. Chen, *J. Appl. Phys.* **60**, 3172 (1986).
- ⁶P. Revesz, J. Gyimesi, and E. Zsoldos, *J. Appl. Phys.* **54**, 1860 (1983).
- ⁷I. C. Wu, Master of Science thesis, National Tsing Hua University, Hsinchu, Taiwan, Republic of China, 1986.
- ⁸J. W. Edington, *Practical Electron Microscopy in Materials Science* (Macmillan, London, 1976).
- ⁹D. W. Lynch and W. R. Hunter, in *Handbook of Optical Con-*

- stants of Solids*, edited by E. D. Palik (Academic, New York, 1985), p. 275.
- ¹⁰H. Kawarada, I. Ohdomari, and S. Horiuchi, *Proc. Mater. Res. Soc. Symp.* **25**, 429 (1984).
- ¹¹W. B. Pearson, *The Crystal Chemistry and Physics of Materials and Alloys* (Wiley-Interscience, New York, 1972), p. 592.
- ¹²D. W. Lynch and W. R. Hunter, in *Handbook of Optical Constants of Solids*, edited by E. D. Palik (Academic, New York, 1985).
- ¹³W. T. Lin and L. J. Chen, *Appl. Phys. Lett.* **46**, 562 (1985).
- ¹⁴Harrison, *Solid State Theory* (McGraw-Hill, New York, 1976), Chap. II.
- ¹⁵I. Abbati, L. Braicovich, De Michelis, O. Bisi, and R. Rovetta, *Solid State Commun.* **37**, 119 (1981).
- ¹⁶Bisi and C. Calandra, *J. Phys. C* **14**, 5479 (1981).
- ¹⁷I. Nishida and T. Sukada, *J. Phys. Chem. Solids* **39**, 499 (1978).

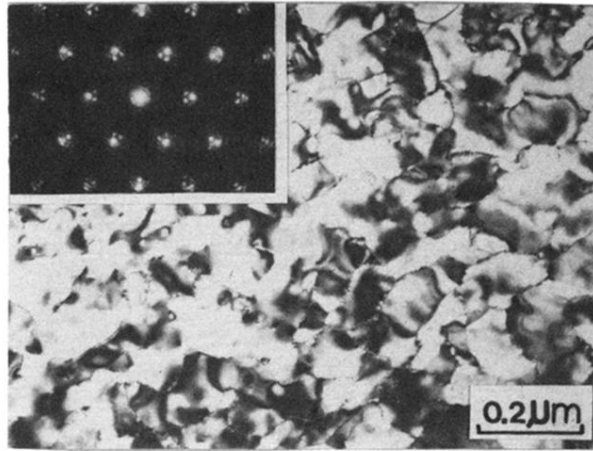


FIG. 2. Bright-field (BF) micrograph of PtSi on Si(111) for 900 °C, 100 s annealed; inset is the diffraction pattern (DP). The grain size is about 8.15 μm .

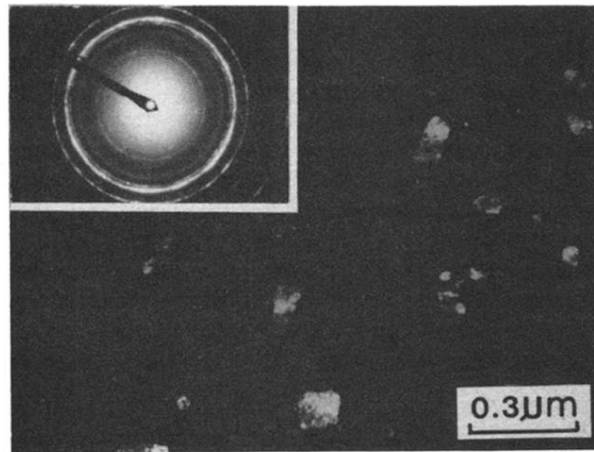


FIG. 5. Dark-field (DF) micrography of CrSi_2 on $\text{Si}(001)$ with grain size of $0.1 \mu\text{m}$; inset is the DP.

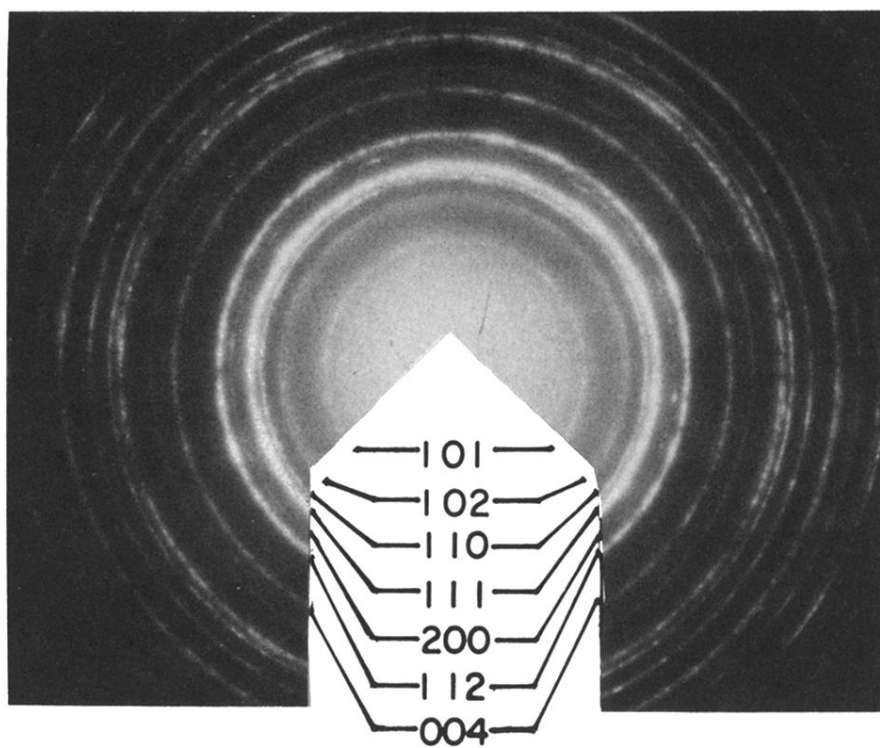


FIG. 6. A typical SAD ring pattern of CrSi_2 (1200 Å)/Si(001) implying an evidence of single phase.

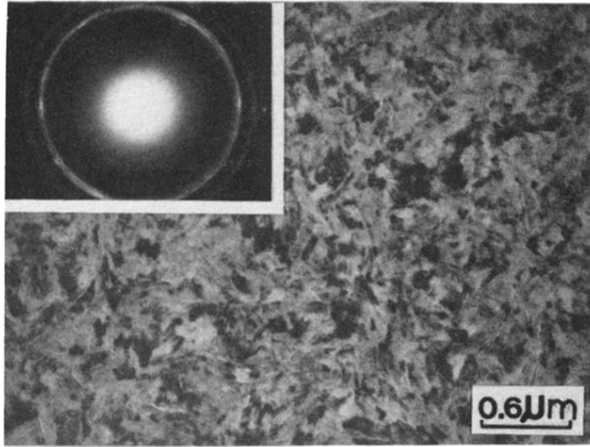


FIG. 9. BF of MoSi₂ on Si(111) with grain size of 1000 Å; the inset is the DP.